http://dx.doi.org/10.5516/NET.02.2013.001

VARIATION OF LOCAL POOL BOILING HEAT TRANSFER COEFFICIENT ON 3-DEGREE INCLINED TUBE SURFACE

MYEONG-GIE KANG
Department of Mechanical Engineering Education, Andong National University 388
Songchun-dong, Andong-city, Kyungbuk 760-749, Korea
E-mail : mgkang@andong.ac.kr

Received June 20, 2013
Accepted for Publication July 30, 2013

Experimental studies on both subcooled and saturated pool boiling of water were performed to obtain local heat transfer coefficients on a 3° inclined tube of 50.8 mm diameter at atmospheric pressure. The local values were determined at every 45° from the very bottom to the uppermost of the tube periphery. The maximum and minimum local coefficients were observed at the azimuthal angles of 0° and 180°, respectively, in saturated water. The locations of the maxima and the minima were dependent on the inclination angle of the tube as well as the degree of subcooling. The major heat transfer mechanisms were considered to be liquid agitation generated by the sliding bubbles and the creation of big size bubbles through bubble coalescence. As a way of quantifying the heat transfer coefficients, an empirical correlation was suggested.

KEYWORDS : Pool Boiling, Subcooling, Local Heat Transfer, Tube, Inclination Angle

1. INTRODUCTION

Mechanisms of pool boiling heat transfer in subcooled and saturated liquid have been studied for a long time. Recently, it has been widely investigated in nuclear power plants for the purpose of acquiring inherent safety functions in case of power supply loss[1,2]. Pool boiling heat transfer is very attractive from the viewpoint of enhancing heat transfer rate in a limited space. Moreover, it can run without the support of any electric pumps. To design more efficient passive heat exchangers, the effects of several parameters on heat transfer must be identified. One of the major issues is the variation of local heat transfer coefficients (h_b) on a horizontal tube. The evaluation of exact values along the tube periphery is important for heat exchanger design.

A study on local heat transfer coefficients on a horizontal tube by Lance and Myers [3] reports that the type of boiling liquid can change the trend of local heat transfer coefficients along the tube periphery. Lance and Myers said that when the liquid was methanol the maximum local heat transfer coefficient was observed at the tube bottom, while the maximum was at the tube sides when the boiling liquid was n-hexane. Moreover, they reported that the difference among the local heat transfer coefficients decreased as the heat flux (q'') increased. Cornwell and Einarsson [4] reported that the maximum local heat transfer coefficient was observed at the tube bottom when the boiling liquid was R113. The location of the maximum heat transfer coefficient moves toward the tube sides as the fluid flow around the tube increases. Cornwell and Houston [5] explained the difference in local heat transfer coefficients along the tube circumference by introducing the effect of sliding bubbles on heat transfer.

According to Gupta et al.'s results [6], when the liquid is water, the maximum and the minimum local heat transfer coefficients are observed at the bottom and top regions of the tube circumference, respectively. Kang [7] reported similar results using the same combination of heated tube diameter and liquid. Gupta et al. studied azimuthal angles (θ) of every 45° along the tube periphery while Kang studied only three angles of 0°, 90°, and 180°. To identify variations in local heat transfer coefficients in detail, Kang [8] studied more azimuthal angles and concluded that the maximum heat transfer was observed at the azimuthal angle of 45°. He also observed that the local heat transfer coefficient measured at θ=90° the average value.

To avoid circumferential temperature distribution on a horizontal tube the application of a porous layer on a part of the heating surface was studied by Dominiczak and Cieslinski [9]. According to the results, the porous layer changes the location of the maximum wall temperature. The lowest temperature on the circumference was recorded within the upper gereratix due to the porous layer. Luke and Golenflo [10] observedthe diameter and frequency of a departure bubble is influenced by the azimuthal position of the active nucleation sites on the tube. Das [11] carried out an experimental investigation and suggested an equation to predict the local pool boiling heat transfer coefficient along the horizontal tube periphery at different pressures. Results by El-Genk and Gao [12] for a hemisphere also said that local heat transfer coefficients were changing along the circumference. Much difference between two

local values at the bottom and sides was observed.

Previous studies on local heat transfer coefficients of a circular shape are summarized in Table 1. Both pool and flow boiling are of concern in the various saturated liquids. Most results are for horizontal tubes of diameter ranging from 7.6~51 mm. One exception is by Sateesh et al. [13]. Sateesh et al. studied variations in local heat transfer coefficients along the tube periphery while controlling the inclination angle (ϕ). They tested five inclination angles (i.e., ϕ=0°, 30°, 45°, 60°, and 90°). The results show that the top wall superheat (ΔT_{sat}) increases and bottom wall superheat decreases as the inclination is changed from 90° to 0° above the horizontal. The cause for the tendency is thought to be the bubble sliding length.

An analytic approach for pool boiling on a surface where the mechanism of sliding bubbles plays an important role has been studied by Sateesh et al. [14]. Through the modeling process they suggested several equations to quantify the effects of natural convection, transient conduction and microlayer evaporation due to stationary bubbles, and transient conduction and microlayer evaporation due to sliding bubbles on pool boiling heat transfer.

Investigation of local heat transfer on a heated tube in subcooled liquid is important when the thermo-hydraulic phenomena are closely related with the integrity of a nuclear reactor [2]. Figure 1 shows a schematic diagram of the passive condensing heat exchanger (PCHX) adopted in the Advanced Power Reactor Plus (APR+). The PCHX cools down the secondary side of a steam generator to eventually remove decay heat from the reactor core. The heat exchanging tubes of the PCHX are inclined 3° from the horizontal position to prevent the occurrence of water hammer. The condition of the water in a passive condensate cooling tank (PCCT), which the PCHX is submerged in,

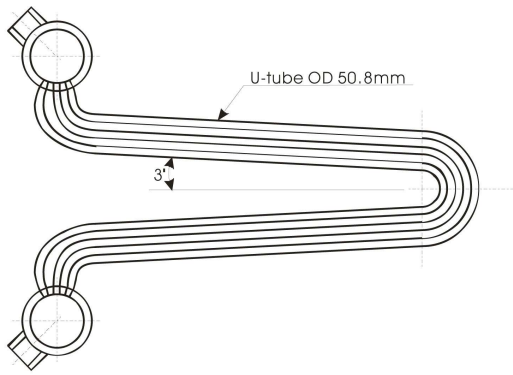

Fig. 1. PCHX Bundle of APR + PAFS[2]

Table 1. Summary of Experimental Conditions in Previous Studies

Author (year)	Tube		Liquid		Boiling condition	ϕ	θ
	material	diameter	type	condition			
Lance & Myers (1958)	copper	31.75mm 50.8mm	Methanol n-hexane	saturated	pool	0°	0°~360°
Cornwell & Einarsson (1990)	stainless steel	27.1mm	R113	saturated	pool flow	0°	0°~360°
Gupta et al. (1995)	stainless steel	19.05mm	water	saturated	pool flow	0°	0°~360°
Luke & Golenflo (2000)	copper steel	7.6mm 8mm	propane	saturated	pool	0°	0°~180°
Kang (2000)	stainless steel	19.05mm	water	saturated	pool	0°	0°~180°
Kang (2005)	stainless steel	51mm	water	saturated	pool	0°	0°~180°
Dominiczak & Clieslinski (2008)	stainless steel	8.15mm 13.52mm 23.60mm	water R141b	saturated	pool	0°	0°~360°
Sateesh et al. (2009)	Stainless steel	21mm 26mm 33mm	water ethanol acetone	saturated	pool	0°~90°	0°, 180°
Das (2010)	copper	31.85mm	water methanol isopropanol	saturated	pool	0°	0°~270°

is first subcooled and becomes saturated as the PCHX operates.

Summarizing the published results, it is necessary (1) to evaluate local heat transfer coefficients on a nearly horizontal tube, and (2) to identify effects of liquid subcooling on local heat transfer coefficients. Therefore, the present study aims to investigate the effects of the inclination angle and liquid subcooling on pool boiling heat transfer. To the author's knowledge, no previous results concerning these effects have been published. The results of this study could provide a clue to the thermal design of the PCHX.

2. EXPERIMENTS

2.1 Experimental Apparatus

A schematic view of the present experimental apparatus and the assembled test section is shown in Fig. 2. The water storage tank is made of stainless steel, with a rectangular cross section (950×1300 mm) and a height of 1400 mm.

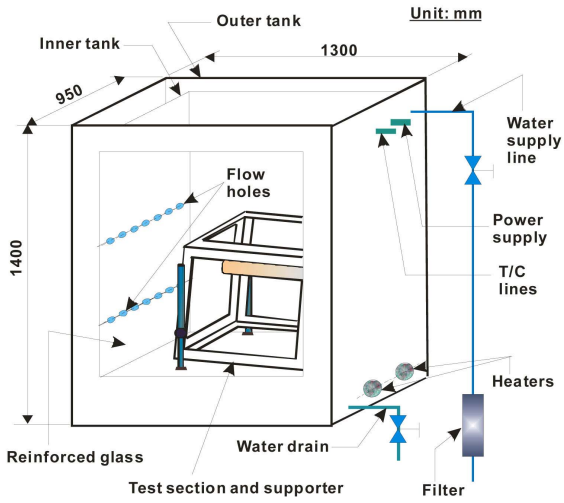

Fig. 2. Schematic Diagram of Experimental Apparatus

This tank has a glass view port (1000×1000 mm) which permits viewing and photography of the tubes inside. The tank has a double container system. The sides of the inner tank are 800×1000×1100 mm (depth×width×height). The bottom side of the inner tank is situated 200 mm above the bottom of the outer tank. Drainage of the inside tank is done by the two passages situated on the bottom side. Outlets of the drain passages are 50 mm above the bottom side of the outer tank to reduce any possible effects of outside fluid on the flow of the inside tank. The inside tank has several flow holes (28 mm in diameter) to allow fluid inflow from the outer tank. To diminish the effects of inflow from outside tank, the holes are situated at 300 and 800 mm above the bottom of the inside tank. Although some areas around the hole can be affected by the inlet flow, it is not expected that the inflow would change the flow characteristics near the heated tube. Four auxiliary heaters (5 kW/heater) are installed in the space between the inside and the outside tank bottoms to boil the water and to maintain the saturated condition. To reduce heat loss to the environment, the left, right, and rear sides of the tank are insulated by fiberglass wool of 50 mm thickness.

The heat exchanger tubes are simulated by a resistance heater (Fig. 3) made of a very smooth stainless steel tube (L =300 mm and D =50.8 mm). Several rows of resistance wires are arrayed uniformly inside the heated tube to supply power to the tube. Moreover, insulation powder is packed into the space between the tube's inner wall and the wires (1) to prevent any possible current flowing to the data acquisition system through the thermocouple lines and (2) to heat the outer stainless steel tube uniformly. The surface of the tube was finished by buffing to have a smooth surface. Electric power is supplied through the bottom side of the tube. To change the azimuthal angle, one side of the test section has a flange. The peripheral variation in heat transfer was determined by rotating the tube following each set of readings. The angular increment between reading positions was 45°. For the test, 220 V AC was used.

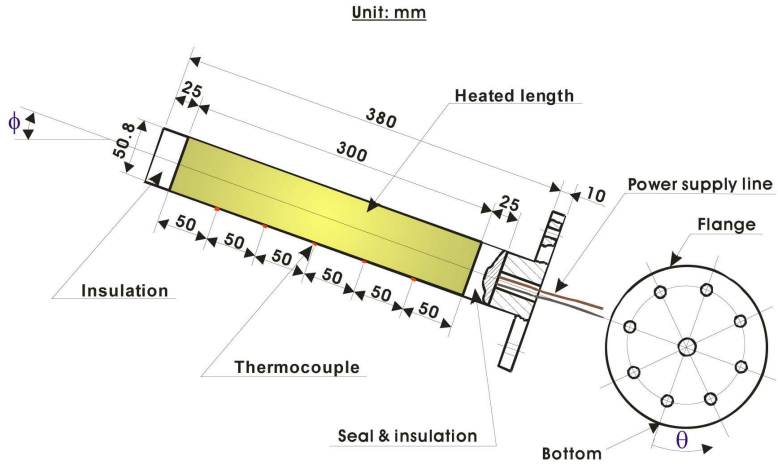

Fig. 3. Test Section and Thermocouple Locations

The tube outside is instrumented with five T-type sheathed thermocouples (diameter 1.5 mm). The thermocouple tip (about 10 mm) is bent at a 90 degree angle and the bent tip brazed on the tube wall. The brazing metal is a kind of brass and the averaged brazing thickness is less than 0.1 mm. The temperature decrease through the brazing metal is calibrated by the one dimensional conduction equation. Since the thermal conductivity of the brass is nearby 130 W/m-ºC at 110ºC [15], the maximum temperature decrease through the brazing metal is 0.08ºC at 100 kW/m^2. The value was calculated by the product of the heat transfer rate and the thermal resistance. The measured temperatures were calibrated considering the above error. The locations of the thermocouples are 50, 100, 150, 200, and 250 mm from the heated tube bottom as shown in Fig. 3. The water temperatures were measured by a rod with six sheathed T-type thermocouples placed vertically at a corner of the inside tank. The thermocouples are brazed on the surface with equal space (i.e., 180 mm) similar to the heated tube. At the bottom side of the rod a small rod of 10 mm diameter was attached to fix it to the tank bottom, which has a hole of the same size. The upper side of the device has a hole to fix it to the tank wall with a bolt and nut. All thermocouples of the heated tube and the device were calibrated at a saturation value (i.e., 100 °C since all the tests were run at atmospheric pressure condition).

To fix the heated tube onto the right position, a supporter was manufactured as shown in Fig. 2. The heated tube and the supporter are assembled by nuts and bolts. To measure and control the supplied voltage and current two power supply systems (each having three channels for reading of voltage and current in digital values) are used. The capacity of each channel is 10 kW.

2.2 Test Process

For the tests, the heat exchanging tube and the tube supporter were assembled and placed at the bottom of the tank. From the start of filling the water storage tank until the initial water level was 1000 mm from the outer tank bottom, the water was heated using four pre-heaters. When the water temperature (T_{wat}) reached the testing point, the supply of electricity to the test tube started and continued until the liquid got to the saturation temperature (T_{sat}). The temperatures of the water and tube surfaces were measured while controlling the heat flux on the tube surface. In this manner a series of experiments was performed for various combinations of the azimuthal angle and liquid condition.

The heat flux from the electrically heated tube surface is calculated from the measured values of the input power as follows:

$$q'' = \frac{q}{A} = \frac{VI}{\pi DL} = h_b(T_s - T_{wat}) = h_b \Delta T \qquad (1)$$

where V and I are the supplied voltage (in volts) and current (in amperes), and D and L are the outside diameter and the length of the heated tube, respectively. T_s and T_{wat} represent the measured temperatures of the tube surface and the water, respectively. The tube and water temperatures used in Eq. (1) are the arithmetic average values of the measured temperatures.

2.3 Uncertainty of the Tests

The uncertainties of the experimental data are calculated from the law of error propagation [16]. The data acquisition error (A_T, ±0.05 °C) and the precision limit (P_T, ±0.1 °C) have been counted for the uncertainty analysis of the temperature. The 95 percent confidence uncertainty of the measured temperature is calculated from $(A_T^2 + P_T^2)^{1/2}$ and has a value of ±0.11 °C. The error bound of the voltage and current meters used for the test is ±0.5% of the measured value. Therefore, the uncertainty of the calculated power (voltage current) has been obtained as ±0.7%. Since the heat flux has the same error bound as the power, the uncertainty in the heat flux is estimated to be ±0.7%. When evaluating the uncertainty of the heat flux, the error of the heat transfer area is not counted since the uncertainty of the tube diameter and the length is ±0.1 mm and its effect on the area is negligible. To determine the uncertainty of the heat transfer coefficient the uncertainty propagation equation has been applied on Eq. (1). Since values of the heat transfer coefficient result from the calculation of $q''/\Delta T$ a statistical analysis on the results has been performed. After calculation and taking the mean of the uncertainties of the propagation errors the uncertainty of the heat transfer coefficient has been calculated as ±6%.

2.4 Analysis on Heat Transfer along the Periphery

Before obtaining local heat transfer coefficients, heat transfer along the tube periphery has been analyzed based on the measured local temperatures at the given azimuthal angles. This kind of approach is necessary to estimate the local coefficients accurately. Lance and Myers [3] used an isolating method to cut off any possible heat transfer to the thermocouple along the tube periphery. For the present study a one dimensional heat conduction analysis was used to estimate the amount of peripheral heat transfer. As the liquid is in saturation and q'' =100 kW/m^2, the maximum temperature difference is 1.7°C between the temperatures at θ =0° and 180°. The one dimensional conduction heat transfer along the tube periphery is calculated as 0.32 kW/m^2. This value is lower than 0.5% of the radial heat flux. Since the amount of peripheral heat transfer is not very large, its effect on the heat transfer coefficient is neglected.

3. RESULTS AND DISCUSSION

3.1 Results

Changes in water temperatures through the vertical height of the tank are shown in Fig. 4. Temperatures measured at four different locations are plotted as a

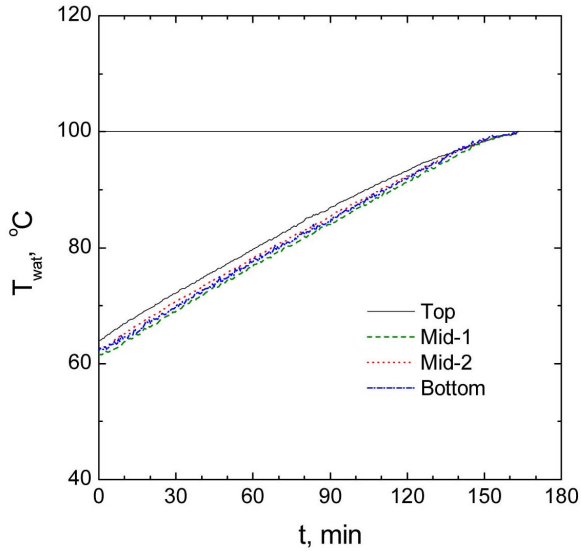

Fig. 4. Variations in Water Temperatures (q'' = 100kW/m², ϕ = 3°)

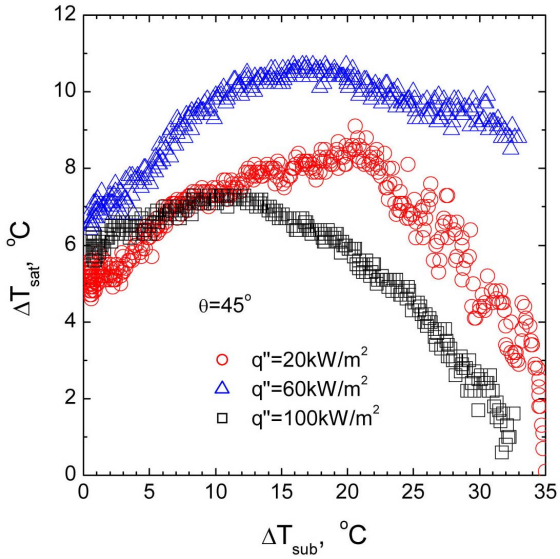

Fig. 5. Plots of ΔT_{sat} Against ΔT_{sub} Data (ϕ = 3°)

function of time (t). The water in the tank is well mixed thermally. The difference between the maximum and the minimum local temperatures is less than 3°C throughout the time duration. The test section is situated near the Mid-2 thermocouple. The local water temperature at this location is almost same as the average water temperature that is used to determine the degree of water subcooling.

Figure 5 shows plots of ΔT_{sat} versus ΔT_{sub} data for θ=45°. The wall superheat ($\Delta T_{sut} = T_s - T_{sat}$) increases for a while and then decreases as the degree of liquid subcooling ($\Delta T_{sub} = T_{sat} - T_{wat}$) increases. This tendency is similar to Judd et al.'s results [17]. The value of ΔT_{sat} increases gradually until ΔT_{sub} reaches 10 °C at q'' =100 kW/m². Then, ΔT_{sat} decreases as the degree of liquid subcooling increases. The ΔT shown in Eq. (1) can be rewritten as $\Delta T_{sat}+\Delta T_{sub}$. That is, $h_b = q''/(\Delta T_{sat}+\Delta T_{sub})$. The values of ΔT_{sat} and ΔT_{sub} represent the conditions of the tube surface and the water, respectively. An increase in ΔT_{sat} enhances the generation of bubbles whereas an increase in ΔT_{sub} suppresses the generation of bubbles. As the liquid becomes saturated, h_b increases suddenly and, then, the value of $\Delta T_{sat}+\Delta T_{sub}$ decreases accordingly.

Some photos of pool boiling on a 3° inclined tube surface are shown in Fig. 6 for different ΔT_{sub} and q''. In highly subcooled liquid the generation and movement of bubbles are very much restricted. At $\Delta T_{sub} \leq 20$ °C bubbles are usually observed on the tube surface only and their size is very small. In this case, the size of a bubble departed from the surface decreases rapidly as it moves to the water level. As the degree of subcooling decreases, the sizes of bubbles moving along the tube periphery increases. At ΔT_{sub} =0 °C the generation of bubble bunches is observed on the tube around θ =180°. The big bubbles are created through coalescence of smaller bubbles. Bubbles coalesce with nearby bubbles when the intensity of liquid agitation

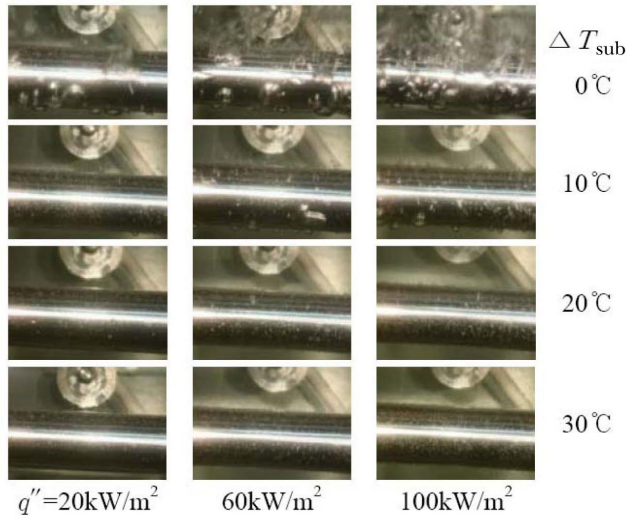

Fig. 6. Photos of Boiling on 3° Inclined Tube Surface

is very weak and/or the density of nucleation sites is increased. At ΔT_{sub} =0~10 °C coalesced bubbles are observed at the bottom side of the tube. As the degree of liquid subcooling decreases, both the density of nucleation sites and the intensity of liquid agitation are increased.

Variations in local heat transfer coefficients on the tube surface against the degree of subcooling are shown in Fig. 7. As ΔT_{sub} increases, a sharp decrease in h_b is observed. When ΔT_{sub} changes from 0°C to 10°C the average heat transfer coefficient decreases about 60.6% (14.57→5.74kW/m²°C) for ϕ =3° and q'' =100kW/m². As ΔT_{sub} increases above 10°C, the rate of change in h_b is decreased. The change of ΔT_{sub} from 10°C to 20°C results in only 37.8% (5.74→3.57kW/m²°C) variation in h_b. The rate of decrease in h_b increases as the heat flux decreases. For ϕ =3° and q'' =100kW/m² the

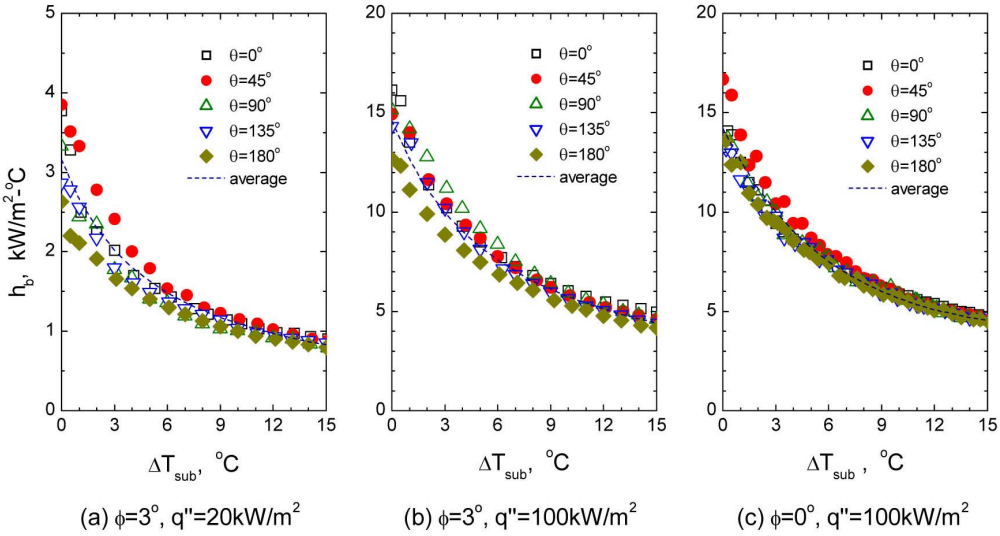

Fig. 7. Plots of h_b Against ΔT_{sub}

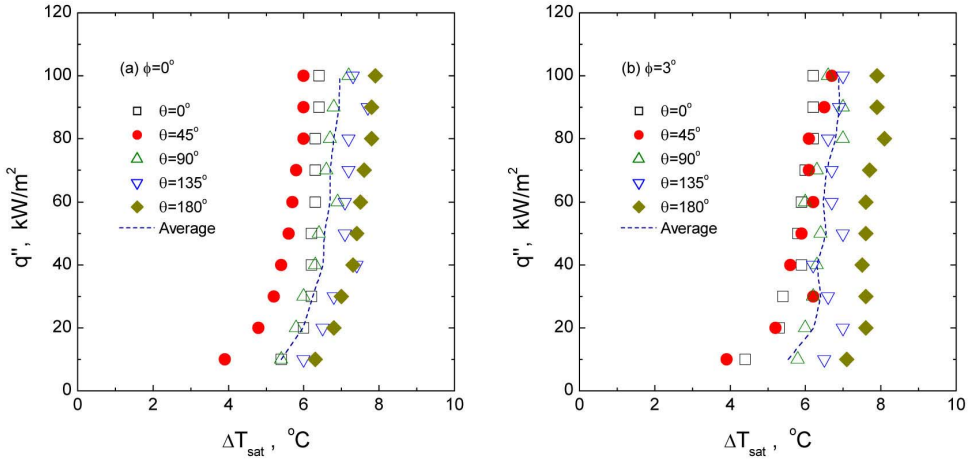

Fig. 8. Plots of q" Against ΔT_{sat}

average heat transfer coefficient reduces 65.2% as ΔT_{sub} changes from 0°C to 10°C. There is no visible difference in the amount and the tendency between the average heat transfer coefficients for the inclination angles of 0° and 3°. However, the azimuthal angle for the maximum heat transfer coefficient changes from 45° to 0° or 90° depending on ΔT_{sub}. For ϕ=3° the change in the heat flux also changes the point of the maximum heat transfer coefficient. The rate of difference between the maximum and the minimum local heat transfer coefficients increases as the inclination angle increases and the heat flux decreases. However, as the degree of water subcooling increases the differences along the local heat transfer coefficients gradually decrease. At 10°C $\leq \Delta T_{sub}$ every local heat transfer coefficient has almost the same value regardless of the inclination angle and the heat flux.

Figure 8 shows plots of q'' versus ΔT_{sat} data as the azimuthal angle changes for the horizontal tube and the 3° inclined tube. The maximum superheat is observed at θ=180° regardless of the inclination angle and the heat flux. However, the minimum superheat depends on the inclination angle and the heat flux. As the tube is inclined by 3°, the minimum ΔT_{sat} is observed at θ=45° while q'' <60kW/m^2. The slope of the experimental data for θ=0° gets steeper when the heat flux is greater than 60kW/m^2. Then, the azimuthal angle for the minimum ΔT_{sat} changes from 45° to 0°. A similar tendency is observed for ϕ=0°. However, the azimuthal angle for the minimum superheat is not changed. Although the average superheats are similar to each other throughout the heat fluxes, there is a slight difference between the superheats for the maxima and the minima. As the inclination angle is changed from 0° to 3° a meaningful difference in ΔT_{sat} is observed at $q'' \leq$ 40kW/m^2. For example, at q'' =10kW/m^2 the difference

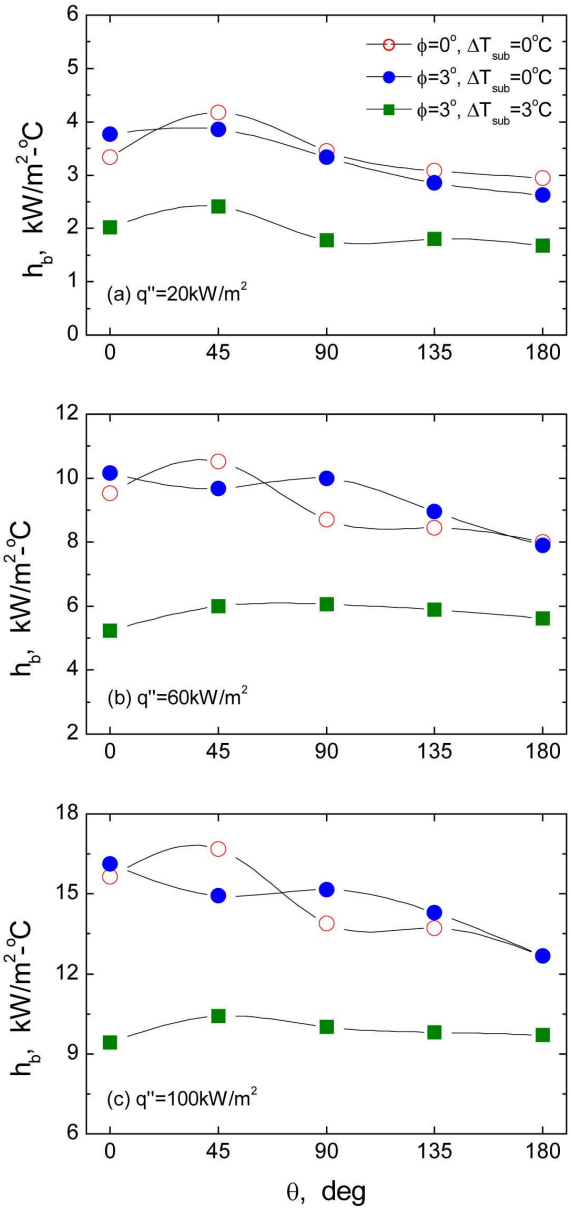

Fig. 9. Peripheral h_b Distribution

between the superheats for the maxima and the minima is 2.4°C for ϕ=0° while it is 3.2°C for ϕ=3°. The causes for this discrepancy can be considered as the bubble sliding length along the tube surface since the only difference between the tubes is the inclination angle.

The peripheral distribution of the local heat transfer coefficient is shown in Fig. 9. The local heat transfer coefficient decreases as the azimuthal angle increases from the bottom (θ=0°) to the top (θ=180°) of the tube circumference. The locations of the maximum and the minimum heat transfer coefficients are dependent on the inclination angle and the degree of subcooling. When the water is saturated (ΔT_{sub}=0°C), the azimuthal angles for the maximum heat

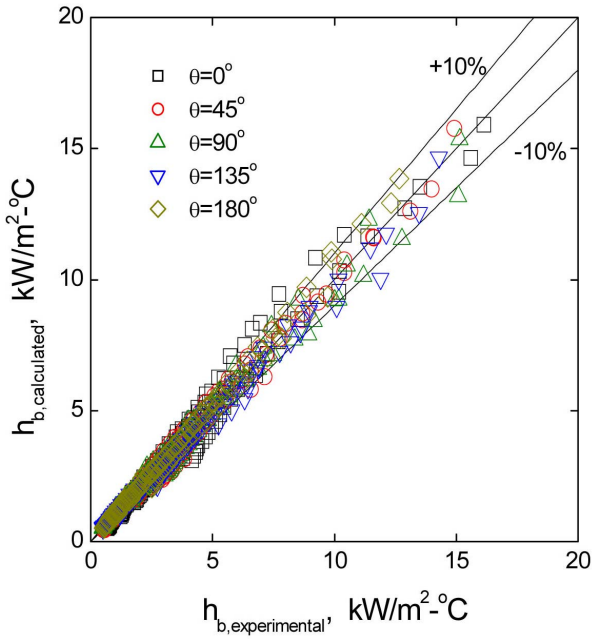

Fig. 10. Comparison of Calculated Heat Transfer Coefficients with Measured Values

transfer coefficient are 45° and 0° for the horizontal tube and the 3° inclined tube, respectively. The azimuthal angle for the minimum heat transfer coefficient is constant regardless of the inclination angle and has a value of 180°. The azimuthal angle for the maximum heat transfer coefficient moves to 45° when ΔT_{sub} is 3°C. Summarizing the tendencies, (1) the variation of ϕ from 0° to 3° changes the azimuthal angle for the maxima from 45° to 0° and (2) an increase in ΔT_{sub} from 0°C to 3°C moves the azimuthal angle for the maxima from 0° to 45°.

To predict the local and average heat transfer coefficients, an empirical correlation has been suggested by using the least-squares method and experimental data gained from the present experiments. The empirical correlation can be correlated as a function of the heat flux and the subcooling as follows:

$$h_b = \frac{q''}{A + B\Delta T_{sub}} \tag{2}$$

where, $A = 6.287\cosh(-0.003\theta)$, $B = 1.096\cos(0.002\theta)$.

The developed correlation predicts the measured experimental data within a ±10% error bound as shown in Fig. 10.

3.2 Discussion

Three heat transfer mechanisms were considered to explain the heat transfer characteristics along the tube periphery as shown in Fig. 11. They are the density of active nucleation sites, sliding bubbles, and bubble coalescence. One of the major causes of the increase in heat transfer coefficients is liquid agitation due to sliding bubbles.

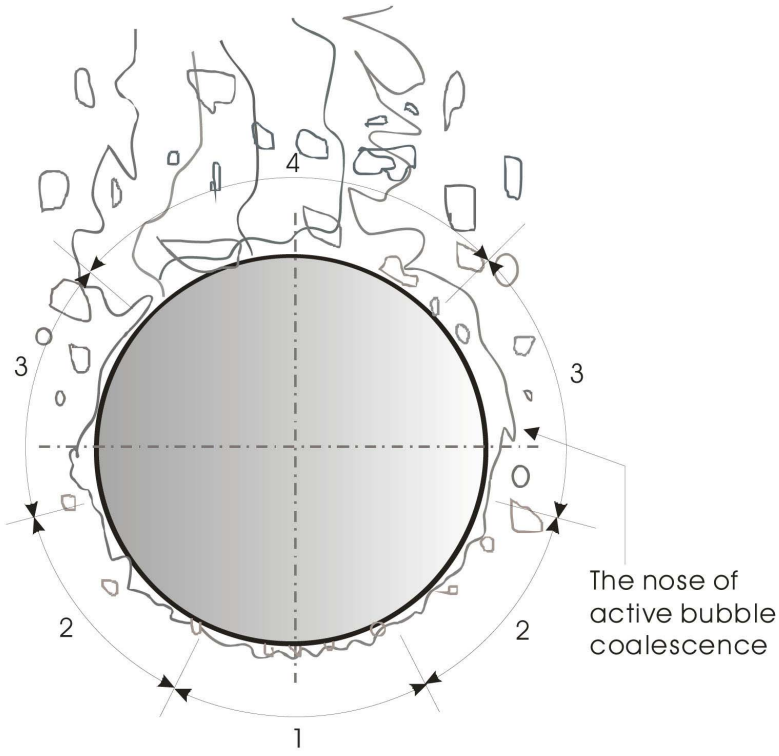

Region Major mechanisms

Region 1: Active nucleation site density
Region 2: Sliding bubbles
Region 3: Sliding bubbles + Bubble coalescence
Region 4: Active bubble coalescence

Fig. 11. Major Boiling Mechanisms Related with Heat Transfer

The mechanisms of transient conduction, microlayer evaporation [14], and the convective bubbly flow due to the sliding bubbles are important for heat transfer enhancement. Moreover, as a bubble moves along the tube periphery, it agitates relevant liquid, disrupts the thermal layer on the surface, and contributes to additional cooling. At θ =45° and ϕ =0°, the intensity of liquid agitation seems to have its largest value since enough moving bubbles are observed and the region is relatively free from bubble coalescence [8]. If the azimuthal angle is larger than 90°, bubbles coming from the lower side start to depart from the surface due to buoyancy and the intensity of liquid agitation decreases. This generates a big bunch of bubbles on the surface. The region of bubble bunches spreads toward the lower side of the tube circumference as the heat flux increases. The coalesced bubbles prevent easy access of relevant liquid to the heated surface and decrease the heat transfer at the upper regions of the tube. The major heat transfer mechanism at this location is microlayer evaporation under stationary bubbles.

At the lowermost region of the tube (θ =0°) a very small amount of active liquid generation is expected at lower heat flux. Therefore, the active nucleation sites can be treated as the major heat transfer mechanism at the lower heat fluxes. Moreover, microlayer evaporation under a stationary bubble can be treated as the important mechanism as the bubble size increases. As the heat flux increases, the number of sites is increased and the rate of flow circulation along the tube also increases. Therefore, the intensity of liquid agitation at the lowermost region gets increased and results in a somewhat sharp increase in the curve slope as shown in Fig. 8.

The azimuthal angle for the maximum heat transfer coefficient is regarded as the location where the effects of liquid agitation and bubble coalescence are high and low, respectively. Therefore, it can be moved to other locations since these two mechanisms are dependent on the inclination angle, the degree of subcooling, and the heat flux. As shown in Fig. 8 and 9 the increases in heat flux and inclination angle move the azimuthal angle for

the maximum heat transfer coefficient to the bottom side of the tube. The nose of active bubble coalescence moves to the bottom side of the tube as the heat flux increases.

As the tube is inclined from the horizontal position, the sliding lengths of bubbles along the tube periphery are increased. The sliding length increases in proportion to $1/\cos\phi$. The bubbles generated at the bottom side of the 3° inclined tube are, then, slightly moved along the bottom regions. Throughout its movement the bubble agitates relevant liquid and becomes the major reason of heat transfer enhancement at the lowermost position for ϕ =3°. Figure 9 shows the changes in heat transfer as the tube inclination is changed from 0° to 3°. Although the azimuthal angle for the minimum heat transfer is constant, the angle for the maximum heat transfer coefficient changes from 45° to 0°.

Since the creation, growth, and departure of bubbles are not easily done in subcooled water, liquid agitation due to rising bubbles is very weak. The chance of bubble coalescence is hardly observed as the degree of subcooling gets increased. The experimental results shown in Fig. 7 explain the effects of liquid subcooling on heat transfer coefficients. There is almost no difference among local heat transfer coefficients as the degree of subcooling increases more than 10°C regardless of the inclination angle and the heat flux. One of the clues for this tendency can be observed visually in Fig. 6. In a highly subcooled liquid no active liquid agitation and bubble coalescence are expected. Therefore, the only effective heat transfer mechanism for this case is the density of nucleation sites. The variation of the local heat transfer coefficient throughout the azimuthal angle is shown in Fig. 9. The results for ΔT_{sub} =3°C show that there is no clear difference among the local heat transfer coefficients.

4. CONCLUSIONS

Local heat transfer coefficients on a smooth stainless steel tube of 50.8 mm diameter with 3° inclination have been investigated experimentally both in subcooled and saturated water at atmospheric pressure. The major conclusions of the present study are as follows:

(1) Much variation in local coefficients was observed along the tube periphery. The maximum values are observed at θ =45° and 0° for ϕ =0° and 3°, respectively. The azimuthal angle for the minimum heat transfer coefficient is 180° and is unchanged by the tube inclination. Major causes of the difference are regarded as liquid agitation due to rising bubbles and bubble coalescence.

(2) The increase in ΔT_{sub} from 0°C to 3°C moves the azimuthal angle for the maximum local heat transfer coefficient from 0° to 45°. As the degree of the liquid subcooling increases more than 10°C the difference between local coefficients decreases since the effects of liquid agitation and bubble coalescence on heat transfer coefficients becomes negligible.

(3) An experimental correlation was suggested to predict the local and average heat transfer coefficients on a 3° inclined tube surface. The correlation can predict the experimental data within a ±10% error bound.

ACKNOWLEDGEMENT

This work was supported by a grant from the 2013 (Special) Research (Support) Fund of Andong National University.

REFERENCES

[1] M. H. Chun and M. G. Kang, "Effects of Heat Exchanger Tube Parameters on Nucleate Pool Boiling Heat Transfer," *ASME J. Heat Transfer*, vol. 120, pp. 468-476 (1998).

[2] K. H. Kang, S. Kim, B. U. Bae, Y. J. Cho, Y. S. Park, and B. J. Yun, Separate and Integral Effect Tests for Validation of Cooling and Operational Performance of the APR+ Passive Auxiliary Feedwater System," *Nuclear Engineering and Technology*, vol. 44, pp. 597-610 (2012).

[3] R.P. Lance and J.E. Myers, "Local Boiling Coefficients on a Horizontal Tube," *A.I.Ch.E. Journal*, vol. 4, pp. 75-80 (1958).

[4] K. Cornwell and J.G. Einarsson, "Influence of Fluid Flow on Nucleate Boiling from a Tube," *Experimental Heat Transfer*, vol. 3, pp. 101-116 (1990).

[5] K. Cornwell and S.D. Houston, "Nucleate Pool Boiling on Horizontal Tubes: a Convection-Based Correlation, *Int. J. Heat Mass Transfer*," vol. 37, pp. 303-309 (1994).

[6] A. Gupta, J.S. Saini, and H.K. Varma, "Boiling Heat Transfer in Small Horizontal Tube Bundles at Low Cross-flow Velocities," *Int. J. Heat Mass Transfer*, vol. 38, pp. 599-605 (1995).

[7] M.G. Kang, "Effect of Tube Inclination on Pool Boiling Heat Transfer," *ASME J. Heat Transfer*, vol. 122, pp. 188-192 (2000).

[8] M.G. Kang, "Local Pool Boiling Coefficients on the Outside Surface of a Horizontal Tube," *ASME J. Heat Transfer*, vol. 127, pp. 949-953 (2005).

[9] P. R. Dominiczak and J. T. Cieslinski, "Circumferential Temperature Distribution during Nucleate Pool Boiling outside Smooth and Modified Horizontal Tubes," *Experimental Thermal and Fluid Science*, vol. 33, pp. 173-177 (2008).

[10] A. Luke and D. Gorenflo, "Heat Transfer and Size Distribution of Active Nucleation sites in Boiling Propane outside a Tube," *Int. J. Therm. Sci*., vol. 39, pp. 919-930 (2000).

[11] M. K. Das, "Study of Local Heat Transfer of Saturated Liquids," *Proceedings of the 37th International & 4th National Conference on Fluid Mechanics and Fluid Power*, Chennai, India, Dec. 16-18, 2010.

[12] M. S. El-Genk and C. Gao, "Experiments on Pool Boiling of Water from Downward- Facing Hemispheres," *Nuclear Technology*, vol. 125, pp.52-69 (1999).

[13] G. Sateesh, S.K. Das, and A.R. Balakrishnan, "Experimental Studies on the Effect of Tube Inclination on Nucleate Pool Boiling," *Heat Mass Transfer*, vol. 45, pp. 1493-1502 (2009).

[14] G. Sateesh, S.K. Das, and A.R. Balakrishnan, "Aanalysis

of Pool Boiling Heat Transfe: Effects of Bubbles Sliding on the Haeting Surface," *Int. J. Heat Mass Transfer*, vol. 48, pp. 1543-1553 (2005).
[15] J.P. Holman, *Heat Transfer*, 8th Ed., McGraw-Hill (1997).
[16] H.W. Coleman and W.G. Steele, *Experimentation and Uncertainty Analysis for Engineers*, 2nd Ed., John Wiley & Sons (1999).
[17] R. L. Judd, H. Merte, Jr., and M. E. Ulucakli, "Variation of Superheat with Subcooling in Nucleate Pool Boiling," *ASME J. Heat Transfer*, vol. 113, pp. 201-208 (1991).